Manuscript published in *J. Agric. Food Chem.* **2021,** *69*, 11322–11335.

In vitro metabolism of azaspiracid-1–3 with a hepatopancreatic fraction from blue mussels (*Mytilus edulis*)

Morten Sandvik[1], Christopher O. Miles[1,2], Kjersti E. Løvberg[1], Fedor Kryuchkov[1], Elliott J. Wright,[2] Elizabeth M. Mudge[2], Jane Kilcoyne[3] and Ingunn A. Samdal[1,*]

[1]Norwegian Veterinary Institute, P.O. Box 64, N-1431 Ås, Norway

[2]Biotoxin Metrology, National Research Council Canada, Halifax, NS, B3H 3Z1, Canada

[3]Marine Institute, Rinville, Oranmore, County Galway H91 R673, Ireland

*Author to whom correspondence should be addressed:

Phone +47 911 79 138

Email: ingunn.samdal@vetinst.no

ABSTRACT

Azaspiracids (AZAs) are a group of biotoxins produced by the marine dinoflagellates *Azadinium* and *Amphidoma* spp. that can accumulate in shellfish and cause food poisoning in humans. Of the 60 AZAs identified, levels of AZA1, AZA2 and AZA3 are regulated in shellfish as a food safety measure, based on occurrence and toxicity. Information about the metabolism of AZAs in shellfish is limited. Therefore, a fraction of blue mussel hepatopancreas was made to study the metabolism of AZA1–3 in vitro. A range of AZA metabolites were detected by LC–HRMS/MS analysis, most notably the novel 22α-hydroxymethylAZAs AZA65 and AZA66, which were also detected in naturally-contaminated mussels. These appear to be the first intermediates in the metabolic conversion of AZA1 and AZA2 to their corresponding 22α-carboxyAZAs (AZA17 and AZA19). α-Hydroxylation at C-23 was also a prominent metabolic pathway, producing AZA8, AZA12 and AZA5 as major metabolites of AZA1–3, respectively, and AZA67 and AZA68 as minor metabolites via double-hydroxylation of AZA1 and AZA2, but only low levels of 3β-hydroxylation were observed in this study. In vitro generation of algal toxin metabolites, such as AZA3, AZA5, AZA6, AZA8, AZA12, AZA17, AZA19, AZA65 and AZA66 that would otherwise have to be laboriously purified from shellfish, has the potential to be used for production of standards for analytical and toxicological studies.

KEYWORDS: azaspiracid; AZA; LC–HRMS; shellfish toxin; mussel; metabolism; hepatopancreas

INTRODUCTION

Azaspiracids (AZAs) were first identified after a food poisoning incident in 1995, when at least eight people in the Netherlands became ill after eating blue mussels (*Mytilus edulis*) harvested at Killary Harbour, Ireland.[1] Symptoms were similar to those of diarrhetic shellfish poisoning (DSP), but the levels of the major DSP toxins (okadaic acid and dinophysistoxin-1 and -2) were very low.[1] Another six poisoning episodes occurred in Ireland, Italy, France, the UK and the USA between 1995 and 2008.[2] A new lipophilic toxin, azaspiracid (AZA1), was isolated, identified and reported in 1998,[3] and in 2004 an expert consultation panel on behalf of FAO/IOC/WHO recommended classifying the AZAs as a separate toxin family.[4] The structures of AZAs (Figure 1) differ from other nitrogen-containing toxins found in shellfish or dinoflagellates by having two unique spiro ring assemblies, a cyclic amine and a carboxylic acid.[3, 5] The original published structure has been revised twice, by Nicolaou et al.[6-7] and more recently by Kenton et al.[8-9]

A series of AZA-analogues have since then been identified.[10-12] AZAs are produced by dinoflagellates of the genera *Azadinium* and *Amphidoma*,[13-16] but can be metabolized to new AZA analogues when consumed by filter-feeding shellfish.[17] AZA-analogues have been identified in European shellfish, such as mussels, scallops, oysters, clams and cockles,[18-22] as well as in brown crabs.[23] In addition to Europe, AZAs have also been reported in shellfish from north-west Africa,[24] Canada,[25] Chile,[26-27] China,[28] the USA[29] and in a sponge from Japan,[30] confirming AZAs to be globally distributed.

The mechanism of action of AZAs, with respect to human toxicity, is still not fully understood,[31] although studies indicate widespread organ damage and tumours in mice,[32-34] teratogenic effects in finfish[35] and modulation of calcium concentrations in human lymphocytes.[36] AZAs have been shown to be K^+ channel blockers,[37] however, the concentrations required are two-fold those for cytotoxicity.

AZA1 and -2 (Figure 1) are produced by *Azadinium spinosum*, *Azadinium poporum* and *Amphidoma languida* and are metabolized by mussels to form a range of other AZAs. Of these, only the levels of AZA1, AZA2, and one of the metabolites (AZA3), are regulated in shellfish.[17] AZA3 is formed via oxidation of the 22-Me of AZA1 to form AZA17 followed by spontaneous decarboxylation to AZA3, and an equivalent process produces AZA6[38] from AZA2 via AZA19. A number of studies have demonstrated this metabolism in shellfish by feeding mussels (*M. edulis*) with cultures of *Az. spinosum*,[39-41] and purified AZA1.[39, 42] A further study fed both mussels (*Mytilus galloprovincialis*) and scallops (*Chlamys farreri*) with cultures of *Az. poporum*[43] and showed that AZA metabolism in scallops differs from that observed in mussels. These studies in shellfish, and analyses of naturally-contaminated shellfish, indicate carboxylation of a methyl group (in mussels, the 22-Me group) to be one of the most prominent metabolic pathways. This, together with insertions of 3β- and 23α-hydroxy groups via oxidative metabolism, and the above-mentioned abiotic decarboxylation of the 22α-carboxyAZAs that are formed, account for the production of AZA3–17, AZA19, AZA21, and AZA23 (Figure 1) from AZA1 and AZA2.[17] An additional metabolic pathway in mussels (*M. edulis*) was reported via esterification of 3β-hydroxyAZAs (e.g., AZA4), although the most abundant AZA ester constituted less than 3% of the sum of the major free AZA analogues.[44] Much less information is available on the mammalian metabolism of AZAs. A study of the metabolism of AZA1 in rat hepatocytes revealed the production of twelve partially characterized oxidized metabolites formed by insertion of up to three oxygen atoms, two metabolites formed by loss of hydrogen, and two putative glucuronic acid (GlcA) conjugates, one of which was tentatively identified as being AZA1 esterified at C-1 by GlcA.[45] No glutathione conjugates were detected in that study, nor were any GlcA conjugates of oxidized AZAs reported.[45]

AZA1–3 are regulated to a maximum permitted level of 160 μg/kg AZA1 equivalents in live bivalve molluscs by the EU to protect human consumers.[46-47] The Codex Alimentarius has adopted the same regulation internationally.[48] The CONTAM Panel established an acute

reference dose (ARfD) of 0.2 μg/kg of AZA1 equivalents and stated "In order for a 60 kg adult to avoid exceeding the ARfD, a 400 g portion of shellfish should not contain more than 12 μg AZA1 equivalents, i.e., 30 μg/kg AZA1 equivalents shellfish meat."[49] The analysis of heat-treated shellfish from Ireland, naturally contaminated with AZAs, revealed high levels of AZA3 (at up to four times the levels of AZA1) and AZA6 (at up to 3 times the levels of AZA2) due to heat-promoted decarboxylation of AZA17 and AZA19, which were not analysed for in the uncooked shellfish.[50] This highlights the fact that AZA1 equivalent values can be grossly underestimated when raw tissues are analysed, as stipulated in the current regulations. Furthermore, in some countries, AZA2 has been reported to be the predominant AZA,[24, 30, 51] and therefore levels of AZA6 will likely be higher in cooked shellfish from these areas. These findings underscore the need for AZA6 to be included in the regulation of AZAs.[50]

Currently, isolation of the minor AZA analogues, including AZA3 and AZA6, for use in toxicological studies and for the preparation of analytical standards, can only be performed from shellfish.[52] In this study, we report the detection of known and new metabolites of AZAs following in vitro exposure of purified AZA1–3 to fractionated mussel (*M. edulis*) hepatopancreas (HP). The goal of this work was to mimic mussel metabolism with a view to producing AZA metabolites (e.g., AZA3 and AZA6) in a cleaner matrix, thereby facilitating access to purified metabolites for the production of analytical standards.

MATERIALS AND METHODS

Materials

AZA1–3 (Figure S1) were from the Marine Institute, Ireland.[52] Nicotinamide adenine dinucleotide phosphate (NADPH) was from Roche (Basel, Switzerland). All other inorganic chemicals and organic solvents were of analytical grade or better. Reference materials of AZA4–10,[53] AZA33, and AZA34[54] were available from earlier work, with AZA11 also present as a contaminant in the standard of AZA10.[53] NRC CRM-AZA-Mus[55] and NRC CRM-FDMT1[56] were from National Research Council Canada (Halifax, NS, Canada), and mussels were

harvested at Bruckless (Donegal Bay, Ireland) in 2005.[52] NRC CRM-FDMT1 was extracted and concentrated by SPE as described by Wright and McCarron [57] NRC CRM-AZA-Mus was extracted using a four-step extraction procedure (method B of McCarron, et al. [55]). The Bruckless mussel tissue (2 g) was homogenized with 5 mL of MeOH using an Omni-prep homogenizer (Omni Int., Kennesaw, GA), the homogenate was centrifuged, and the supernatant filtered through a Titan3 cellulose syringe filter (0.45 µm; ThermoFisher Scientific, Rockwood, TN) and then a Millipore 0.45 µm PVDF spin filter (Merck Millipore, Cork, Ireland).

Preparation of the hepatopancreatic fraction from mussels (*M. edulis*)

Mussels were obtained from Snadder og Snaskum (Rissa, Norway). HP (digestive gland) was excised from the blue mussels and pooled. All preparations were prepared on ice or under cooling. The HP-tissue (2 vials of 4.2 g) was homogenized in sodium phosphate buffer (15 mL; pH 7.5; 0.1 M) containing 0.15 M KCl, 10% glycerol, 1 mM EDTA and 1 mM D,L-dithiothreitol using an Ultra Turrax T25 (IKA, Staufen, Germany) for ~1 min, until homogenous, in centrifuge tubes. The homogenate was centrifuged (39,200 *g*; 4 °C; 25 min (J2-MC, Beckman Instruments, Palo Alto, CA)). The supernatants (HP-fractions) were transferred to microtubes in aliquots and stored at −80 °C. Total protein in the HP-fractions was determined by modified Lowry assay[58] to be 16.9 mg/mL.

In vitro metabolism experiments

Metabolism experiments were performed with six replicates in 15-mL glass vials by combining 1.34 mL sodium phosphate buffer (0.1 M; pH 7.5) with 100 µL of the prepared HP-fraction and 10 µL of AZA1 (557 ng/mL), AZA2 (543 ng/mL) or AZA3 (458 ng/mL) in MeOH. The metabolic reactions were initiated by addition of the co-factor NADPH (50 µL; 20 mM). The incubations were performed at 21–25 °C in a shaking water bath (Grant OLS200, Grant Instruments, Shepreth, Royston, UK). Of the six replicates for each AZA, three were incubated for 30 min, and three for 20 h.

In parallel, four control experiments (i–iv) were also performed: i, sodium phosphate buffer, HP-fraction, AZA1, and NADPH; ii, sodium phosphate buffer, HP-fraction, and NADPH; iii, sodium phosphate buffer, HP-fraction, and AZA1, and; (iv) sodium phosphate buffer, HP-fraction preheated to 60 °C for 2 min to deactivate it, AZA1, and NADPH. These control experiments were stopped immediately (at time 0 min). Additionally, twelve control incubations were performed, four for each AZA1–3 in sodium phosphate buffer in the shaking water bath, as follows: (a) with NADPH, and incubated for 30 min; (b) without NADPH, and incubated for 30 min; (c) with NADPH, and incubated for 20 h, and; (d) without NADPH, and incubated for 20 h.

All reactions were stopped by addition of 1.5 mL ice-cold MeCN and the vials were centrifuged at 1750 *g* for 30 min at 4 °C (Jouan BR4i; ThermoFisher Scientific, Waltham, MA). The supernatants were transferred to Spin-X vials (0.22 µm; Costar, Washington, D.C.) and centrifuged at 7500 *g* for 1 min at ambient temperature (Eppendorf centrifuge 5415D, Hamburg, Germany), and the filtrates transferred to HPLC -vials and stored at −20 °C.

Liquid chromatography–high-resolution tandem mass spectrometry (LC–HRMS/MS) Analysis

Method A. LC–HRMS/MS analysis was performed on a Q Exactive-HF Orbitrap mass spectrometer equipped with a HESI-II heated electrospray ionization interface (ThermoFisher Scientific, Waltham, MA) using an Agilent 1200 LC system including a binary pump, autosampler and column oven (Agilent, Santa Clara, CA). Analyses were performed with a Symmetry Shield 3.5 µm C18 column (150 × 2.1 mm; Waters, Milford, MA) held at 40 °C with mobile phases A and B of H_2O and MeCN, respectively, each of which contained formic acid (0.1% v/v). Gradient elution (0.3 mL/min) was from 30–55% B over 20 min, then to 100% B over 0.1 min and held at 100% B (1 min), then returned to 30% B over 0.1 min and held at 30% B (3.9 min) to equilibrate the column (total run time 25 min). Injection volume was 1–5 µL.

The MS was operated in positive and negative ionization (calibrated from *m*/*z* 74–1622, and *m*/*z* 69–1780, respectively) modes. The spray voltage was 3.7 kV, the capillary temperature was 350 °C, and the sheath and auxiliary gas flow rates were 25 and 8 units, respectively, with MS data acquired from 2–20 min. Mass spectral data was collected using a full-scan (FS) method with alternating positive and negative mode scan data collected from *m*/*z* 700–1100 using the 60,000-resolution setting, an automatic gain control (AGC) target of 1×10^6 and a maximum injection time (max IT) of 120 ms.

Putative AZAs detected using the above FS method were further probed in a targeted manner with positive ionization using alternating FS and parallel reaction monitoring (PRM) scan modes. The settings were as above, except that the FS was scanned from *m*/*z* 700–1050 and max IT was set to 100 ms. The PRM scans were obtained with the low mass set to 60, a 0.7 *m*/*z* precursor isolation window, the 15,000-resolution setting, an AGC target of 2×10^5 and a max IT of 3000 ms, using a stepped collision energy (CE) of 60, 65 and 70 eV. Where chromatographic separation was sufficient, the PRM scans were scheduled, but where peak overlap and signal intensity considerations prevented this, PRM scans were obtained from multiple injections of the sample.

Method B. LC–HRMS was conducted with the same LC–HRMS system (in positive mode, and calibrated as above) as for LC–HRMS method A. An Agilent Poroshell 120 SB-C18 column (2.7 μm, 150 × 2.1 mm) was held at 40 °C and eluted (0.275 mL/min) with mobile phases consisting of H_2O (A) and 95% MeCN (B), each containing 50 mM formic acid and 2 mM ammonium formate. Gradient elution was from 5% to 100% B over 20 min, then held for 7 min while flow rate was linearly increased to 0.6 mL/min, held for 11 min, then returned to 5% B over 1 min, and re-equilibrated for 10 min, with 1 μL injections and the mobile phase diverted to waste for the first 6 min. Source conditions for the mass spectrometer were: spray voltage 3 kV, capillary temperature 350 °C, sheath and auxiliary gas 35 and 10 arbitrary units, with the probe heater set to 300 °C, and S-Lens RF Level 50. Full-scan with data-dependent MS/MS were

acquired with FS at the 60,000 resolution setting, 1×10^6 AGC target, max IT 50 ms, and *m*/*z* scanned from 600–1600. The ten most intense ions above the 5×10^4 intensity threshold were sampled from each FS spectrum for MS/MS, acquired at the 15,000 resolution setting, with AGC target 2×10^5, max IT 60 ms, with a stepped CE of 35 and 60 eV, using the apex trigger function (3–30 s), dynamic exclusion of 3.5 s, and isotope exclusion. An inclusion list containing exact masses of $[M+H]^+$ for previously reported AZAs was used (3 ppm tolerance) along with an exclusion list containing the top 50 most intense background ions in each 2-minute interval across the chromatographic run. The FS with PRM data were obtained with FS using the 120,000 resolution setting, 3×10^6 AGC target, max IT 200 ms, *m*/*z* range of 200–2000, and the MS/MS spectra were acquired with an isolation window of 0.4 Da on precursor masses using the 30,000 resolution setting, AGC target 2×10^5, max IT 100 ms and CE of 55 eV.

Method C. LC–HRMS was conducted with the same LC–HRMS system (in positive mode, and calibrated as above) as for LC–HRMS (method A). Separations used a C8 column (1.9 μm, 100 × 2.1 mm, Thermo Hypersil Gold; Thermo Fischer Scientific, Waltham, MA) with gradient elution. The mobile phase was water (A) and 95% MeCN (B), each containing 50 mM formic acid and 2 mM ammonium formate. The elution gradient (0.25 mL/min) was: 0–5 min, 50–100% B; 5–20 min, 100% B; 20–20.1 min, 100–50% B; and 5 min re-equilibration at 50% B. The column and sample compartments were maintained at 20 °C and 10 °C, respectively and the injection volume was 5 μL. Full-scan spectra were collected with the 60,000 resolution setting, from *m*/*z* 650–1200 using positive ionization with a spray voltage of 3 kV. The sheath gas pressure was 35 psi and auxiliary gas flow was 10 (arbitrary units), the capillary temperature was 350 °C, and the heater was at 300 °C. The AGC target was 1×10^6 and the max IT was 200 ms.

Data-independent acquisition was used to screen for AZA-esters, using fifteen mass windows of 39 Da spanned the range from *m*/*z* 650–1200 with a CE of 80 eV to collect product ion spectra from all ions within each window. The MS resolution was set at 15,000 with an AGC target of 2

217 $\times 10^5$, a max IT of 50 ms, and a loop count of 8. Data-dependent acquisition (DDA) was used to
218 collect MS/MS product ion scans of the five most abundant ions in the full-scan acquisition at
219 each cycle. The mass range for full-scan acquisition was *m*/*z* 750–1250 with a resolution setting
220 of 60,000, an AGC target of 1×10^6, and a max IT of 100 ms.

221 **RESULTS AND DISCUSSION**

222 Hepatocyte-like fractions were prepared from blue mussel HP to study the metabolism
223 of AZAs and evaluate the feasibility of producing metabolite standards in vitro. Progress of the
224 metabolism of AZA1–3 was monitored by LC–HRMS (method A) at 30 min and 20 h of
225 incubation (Table 1, Figure 2). Metabolite identities were established by examination of their
226 HRMS/MS spectra and comparison of these with the literature, the metabolites' relative retention
227 times and the accurate masses of their $[M+H]^+$ ions and, where available, comparison with
228 retention times and HRMS/MS spectra of authentic standards. In a preliminary experiment, in
229 which almost identical results were obtained as in the experiment reported here, incubations were
230 terminated by addition of ice-cold MeOH. This resulted in the formation of small amounts of
231 methyl ketals (at C-21) and methyl esters (at C-1) of the AZAs and their metabolites,
232 complicating the LC–HRMS analysis and data interpretation. To avoid this, incubations were
233 terminated by addition of ice-cold MeCN in all subsequent experiments. No new AZAs were
234 detected by LC–HRMS (method A) in any of the control samples, and their AZA-profiles at all
235 time points were indistinguishable from those of the stock solutions, showing that NADPH and
236 the hepatopancreatic fraction were required for the observed transformations of AZA1–3.

237 LC–HRMS analysis showed that less than 8% conversion of AZA1 and AZA2 to
238 detectable metabolites had occurred by 30 min incubation time, whereas approximately 12% of
239 AZA3 had been converted at 30 min, primarily to AZA5. However, by 20 h, AZA1 and AZA3
240 had undergone ~70–90% conversion to metabolites, while AZA2 had undergone ~50–60%
241 conversion (Table 1, Figure 2). These results suggest that the order of susceptibility to
242 metabolism in the in vitro system used in this study is AZA3 > AZA1 > AZA2, although the

differences were not large. Because the 30-min incubations did not display a high degree of metabolic conversion, only the 20-h incubations were examined in detail for their metabolite profiles. Recently-identified AZA-esters in mussel tissues have been shown to elute much later in the chromatographic analysis.[44] The metabolism samples were also evaluated according to this AZA-ester screening method (LC–HRMS method C), but only product ions characteristic of unesterified AZAs were observed early in the chromatograms, with no sign of their late-eluting esters, in both data-dependent (Figure S2) and data-independent acquisitions. This shows that AZA-esters were not produced in detectable amounts in this metabolism study.

The mass spectral fragmentation patterns of AZAs (Figure 3) in positive ionization mode are structurally diagnostic and can be used as an aid to structure elucidation. For example, cleavage A (Figure 3) is only significant when R^3 (Figure 1) is a hydroxy group, such as in AZA4, AZA7, AZA9 (Figure S3), AZA11 and AZA13–16,[53, 59] cleavage B is a retro-Diels–Alder cleavage and requires the presence of the 7,8-double bond, cleavage E has been reported for 22α-carboxyAZAs such as AZA17, AZA19, AZA21, and AZA23,[59] and cleavages F and H are characteristic of 23α-hydroxyAZAs (Figure 1, R^4 = OH) such as AZA5, AZA8, AZA10 and AZA12–16.[53, 59] Cleavage G is generally regarded as being characteristic of AZAs,[17] but it presumably requires the presence of either a 21-OH group or a 21,22-double bond to produce this retro-Diels–Alder cleavage, while cleavages I–K appear in most AZAs since they involve a substructure common to almost all AZAs reported to date.[17, 60] Analysis of the corresponding fragmentation patterns of AZAs for which standards were not available (AZA12–17, AZA19, AZA21, AZA23, AZA65–68, AZA(872), AZA(886), and AZA(858)) was used to help define, or partially define, the structures of the other AZAs reported in Table 1 and Figure 1.

Metabolites from AZA1. All three replicates showed similar metabolite profiles, with four prominent new earlier-eluting peaks with *m*/*z* values consistent with monohydroxylation (two peaks, *m*/*z* 858.4998), carboxylation at a methyl group (one peak, *m*/*z* 872.4791), and demethylation (one peak, *m*/*z* 828.4893) (Table 1, Figure 2). It was anticipated that these would

correspond to the known AZA metabolites AZA7 and AZA8 (3β- and 23α-hydroxylation, respectively, of AZA1), AZA17 (oxidation of the 22-CH_3 group of AZA1 to a CO_2H group), and AZA3 (resulting from spontaneous 22-decarboxylation of AZA17) (Figure 4). In addition to these major peaks, numerous small peaks were observed with *m*/*z* values consistent with various degrees of oxidation of AZA1, including hydroxylation, dihydroxylation and insertion of a carbonyl group. Most notable amongst these was a low intensity, but very broad, early-eluting peak with the same *m*/*z* as AZA17 (Figures 2 and S4–S7), referred to hereafter as AZA(872), whose peak area comprised about 10% of the total AZAs identified (Table 1, Figure 2) in this sample (i.e., AZA1, AZA3, AZA5, AZA7, AZA8, AZA17, AZA65, AZA67 and AZA(872)).

Authentic standards of AZA1, AZA3, AZA5, AZA7 and AZA8 were available from previous work, and direct comparison of retention times (Figure S8) and HRMS/MS spectra of the standards verified their identities in the extracts of metabolized AZA1. No standard of AZA17 was available, but this was identified from its HRMS/MS (Figure 5) spectrum, including a characteristic strong neutral loss of CO_2 from all product ions containing C-1–C-22, and relative retention time (before AZA1 and AZA3). Furthermore, in an extract heated at 60 °C for 30 min, the peak of AZA17 essentially disappeared and there was a corresponding increase in the intensity of the peak of AZA3, while the peaks for the other major AZAs in the sample (AZA1, AZA7, AZA8, AZA65, AZA67 and AZA(872) were unaffected (Figure S9). This is consistent with the documented propensity of 22α-carboxyAZAs for spontaneous decarboxylation[38, 42, 50] and, taken together, this evidence confirms the identity of AZA17 in the extract.

The earlier-eluting of the two major hydroxyAZAs, AZA65, did not co-elute with the standard of AZA7 (Figure S8), and its HRMS/MS spectrum (Figure 5) showed characteristic differences to both of the known monohydroxylated metabolites of AZA1 (AZA7 and AZA8) but contained similar features to those of AZA17 (Figure 5). In particular, cleavages A, F and H were not present, excluding the presence of a hydroxy group at C-3 or C-23, but cleavages B, C, D, G and I–K were present. An additional characteristic partial loss of CH_2O (30.0106 Da)

accompanied cleavages B–D, as well as the pseudomolecular ion. This is indicative of the presence of an oxidized methyl group located between C-20 and C-23 and, given that the sample was produced via metabolism of pure AZA1, AZA65 can only be 22α-hydroxymethylAZA3 (AZA65) produced by hydroxylation of the 22-methyl group of AZA1. Thus, the neutral loss of CH_2O from AZA65 is due to cleavage E (Figure 3), and is directly analogous to (albeit less prominent than) the corresponding cleavage (loss of CO_2) in the MS/MS spectrum of AZA17 (Figure 5). The proposed structure of AZA65 as 22α-hydroxymethylAZA3 is also consistent with the complete absence of a corresponding metabolite in the metabolism experiment conducted with AZA3 (see below), because the only structural difference between AZA3 and AZA1 is that the former lacks a 22-methyl group.

The unidentified very early-eluting peak, referred to here as AZA(872), constituted a significant proportion of the identified metabolites of AZA1 and had the same accurate mass as AZA17 (Figure S5). The peak was very broad and non-Gaussian in shape (Figures 2 and S4), and it did not display the *m*/*z* 362.2690 (cleavage G) product ion that is generally considered characteristic of AZAs (Figures 5 and S6), nor did it display a neutral loss of CO_2 that might be expected for a carboxylic acid derivative of AZA1. However, it did show product ions consistent with cleavages I, J and K associated with the C-28–C-40 substructure, confirming that it is an AZA metabolite (Figures 5 and S6). Consideration of the accurate mass of the compound indicates that it contains two extra oxygen atoms, two fewer hydrogen atoms, and one extra ring/double bond equivalent (RDBE), relative to AZA1. These changes all appear to be located between C-16 and C-27, because product ions consistent with cleavages B and C of AZA1, but with the abovementioned changes to the number of hydrogen and oxygen atoms and RDBE, dominated the higher mass region of the MS/MS spectrum (Figures 5 and S6). The major product ion observed at *m*/*z* 434.2907 ($C_{25}H_{40}O_5N^+$, Δ 1.4 ppm) must therefore include C-22–C-40 and appended substituents as well as 7 RDBE, five of which presumably come from the olefinic methylene at C-26 and rings F–I. These features are all consistent with oxidation, possibly

accompanied by ring opening, of the E-ring of AZA1 and the presence of one or more carbonyl groups in AZA(872). The presence of carbonyl groups would be consistent with the broad and irregular peak shape for this compound (Figure S4), since these could undergo keto–enol tautomerization and related isomerizations on-column in the acidic mobile phase used in this study. AZA(872) was also detected in the freeze-dried mussel-tissue reference material (NRC CRM-FDMT1) (Figure S7) which, together with the detection of AZA65 in CRM-FDMT1 (Figure S10), suggests that the metabolism observed in this in vitro study with the Norwegian mussel hepatopancreatic fraction approximates that which occurs in naturally-contaminated Irish mussels, even though the relative proportions of the AZA metabolites differed in the two systems.

One early-eluting peak (AZA67) (Figure 2) was observed with $[M+H]^+$ at *m*/*z* 874.4952 ($C_{47}H_{72}O_{14}N^+$, Δ 0.5 ppm), consistent with a dihydroxylated derivative of AZA1, such as the known mussel metabolite AZA14 (3β,23α-dihydroxyAZA1). The product ion spectrum of this compound (Figure 6) showed ions from cleavages G and I–K, indicating that no hydroxylation had occurred in the C-24–C-40 region. Unexpectedly, the product ion spectrum did not contain ions consistent with cleavage A that would be anticipated if a 3β-hydroxy group was present, but product ions from cleavages B–D indicated dihydroxylation in the C-20–C-23 region. Product ions were also present that were consistent with cleavages F and H (Figures 3 and 6), which are indicative of 23α-hydroxylation. In addition to this, $[M+H]^+$ and the product ions attributable to cleavages B–D all showed additional partial neutral losses of 30.0106 Da (CH_2O) (cleavage E), which indicates the presence of an oxidized methyl group between C-20 and C-23. Thus, AZA67 must be 22α-hydroxymethyl-23α-hydroxyAZA3. The stereochemistry at C-23 can reasonably be assumed to be identical to that of the 23α-hydroxyAZA1 (AZA8) already identified in the same sample. The presence of AZA67 is consistent with the observation that hydroxylation of the 22-Me group was the predominant route of oxidation, followed by 23α-hydroxylation, and that only trace amounts of 3β-hydroxylation occurred with this system.

346 **Metabolites from AZA2**. As with AZA1, little metabolism of AZA2 was observed by
347 LC–HRMS at 30 min (Table 1), but more than 50% conversion of AZA2 had occurred by 20 h
348 (Figure 2). The metabolite profile for AZA2 was essentially identical to that of AZA1, except
349 that the metabolites of AZA2 all contained an 8-Me group, and thus were 14.0157 Da heavier
350 and eluted 1.3 min later than the corresponding metabolites from AZA1. Again, all three
351 replicates showed similar metabolite profiles, with four new earlier-eluting peaks with $[M+H]^+$
352 *m*/*z* values consistent with monohydroxylation (two peaks, *m*/*z* 872.5155), carboxylation at a
353 methyl group (one peak, *m*/*z* 886.4947), and demethylation (one peak, *m*/*z* 842.5049) (Table 1,
354 Figures 2 and S11). Numerous minor peaks corresponding to oxidized AZA2 were also present,
355 including a broad early-eluting peak with $[M+H]^+$ 886.4947 (AZA(886)), again closely
356 paralleling the metabolism observed for AZA1. An authentic standard of AZA12 (23α-
357 hydroxyAZA2) was not available, and the identity of this metabolite is reported based on
358 comparison of its MS/MS spectrum with the literature.[59] AZA11 was reported as a 4.8%
359 contaminant of AZA10 in the standard prepared by Kilcoyne et al.[53] Careful examination of the
360 HRMS/MS spectra of the two major monohydroxylated AZA2 metabolites indicated that the
361 later-eluting analogue fragmented as expected for AZA12, but that the earlier-eluting analogue
362 did not fragment in a manner consistent with AZA11 (Figures 3 and 7), nor did it co-elute with
363 AZA11 present in the standard of AZA10 (Figure S12). Rather, this metabolite displayed partial
364 losses of 30.0106 Da (CH_2O) (cleavage E) from the pseudomolecular ion and all the product ions
365 attributable to cleavages B–D, did not show cleavages F or H (which result from 23α-
366 hydroxylation), and displayed the characteristic AZA cleavages G and I–K. These results indicate
367 hydroxylation of AZA2 between C-20 and C-23, and can only be accounted for by 22α-
368 hydroxymethylAZA6 (AZA66). Only very low levels of 3β-hydroxyAZA2 (AZA11) were
369 detectable even after 20 h of metabolism. The characteristics of the later-eluting peak with
370 $[M+H]^+$ at *m*/*z* 886.4947 (Figure 2) are consistent with the known mussel metabolite 22α-
371 carboxyAZA3 (AZA19), with fragmentations including neutral losses of CO_2 (cleavage E, Figure

372 3) from $[M+H]^+$ and from product ions associated with cleavages B–D. This was confirmed by
373 the rapid decarboxylation of AZA19 to give AZA6 upon heating of the extract, while the
374 intensities of the peaks for AZA2, AZA11, AZA12, AZA66, AZA68 and AZA(886) were
375 essentially unaffected (Figure S13). The fourth major metabolite from AZA2, with $[M+H]^+$ with
376 *m*/*z* 842.5049 had the same retention time (Figure S11) as, and an identical HRMS/MS spectrum
377 to, 22-demethylAZA2 (AZA6). The very broad early-eluting peak of AZA(886) had the same
378 [M+H] *m*/*z* as AZA19, but did not show any neutral loss of CO_2 in its HRMS/MS spectrum.
379 While its pseudomolecular ion was 14.0157 Da heavier than that of AZA(872) (Figure S5), the
380 remainder of its product ion spectrum was identical to that of AZA(872) (Figure S6), and this,
381 together with its chromatographic characteristics, indicate it to be identical to AZA(872) except
382 for the presence of an 8-methyl group. As was the case with AZA1, metabolism of AZA2 with
383 blue mussel HP-fraction afforded a minor early-eluting peak (Figure 2) with *m*/*z* consistent with
384 $[M+H]^+$ of dihydroxyAZA2 (AZA68). The product ion spectrum of AZA68 (Figure 6) exactly
385 paralleled that of AZA67 except that the *m*/*z* of the product ions was consistent with the presence
386 of an 8-Me group, thus indicating this compound to be 22α-hydroxymethyl-23α-hydroxyAZA6
387 (AZA68). Although a standard of AZA9 (Figure S3), a known metabolite of AZA2 in mussels,
388 was available, AZA9 could not be detected in extracts from the HP-fractions treated with AZA2,
389 presumably due to the low rate of 3β-hydroxylation in this system.

390 **Metabolites from AZA3**. Metabolism of AZA3 was significantly more rapid than for
391 AZA2, with identified metabolites constituting ~10% of the total AZAs in the extracts after 30
392 min (Table 1). By 20 h, the metabolite profile was dominated by 23α-hydroxyAZA3 (AZA5),
393 with much lower levels of 3β-hydroxyAZA3 (AZA4) (Table 1, Figure 2) identified by LC–
394 HRMS/MS (Figure 8) and comparison with reference standards (Figure S14). Although low
395 levels of numerous unidentified oxidized metabolites were present, no carboxy- or demethyl-
396 AZAs were identified. As with AZA1 and AZA2, a very broad early-eluting peak (denoted
397 AZA(858)) was detected, in this case with $[M+H]^+$ *m*/*z* 858.4634. Although this is the same *m*/*z*

value as would be expected for carboxyAZA3, the chromatographic, HRMS and HRMS/MS characteristics of AZA(858) (Figures 8 and S4–S6) closely paralleled those of AZA(872) and AZA(886) discussed above, except that product ions from cleavages B, C and the main product ion detected at *m*/*z* 420.2739 ($C_{24}H_{38}O_5N^+$, Δ -1.3 ppm) from AZA(858) were missing a CH_2 group relative to those from AZA(872). This confirms that the product ions at *m*/*z* 434.2901 in AZA(872) and AZA(886), and at *m*/*z* 420.2744 for AZA(858), contain C-22–C-40 of the AZA skeleton and, as discussed above for the metabolites of AZA1, these three metabolites (AZA(872), AZA(886), and AZA(858)) appear to be analogous, to contain extra carbonyl groups, and are possibly accompanied by ring-opening in the E-ring (C-21–C-25). A minor sharper, early-eluting peak (AZA13), was also present with *m*/*z* 860.4796 ($C_{46}H_{70}O_{14}N^+$, Δ 0.6 ppm) (Figure 2), consistent with a dihydroxylated derivative of AZA3. Examination of the HRMS/MS spectrum of AZA13 (Figure 8) showed the presence of cleavage A, in addition to cleavages F–K, indicating the presence of both 3β- and 23α-hydroxylations on the AZA3 skeleton. The stereochemistries of these oxidations can be assumed to be identical to those demonstrated by the observed formation of AZA8 and traces of AZA7 during the metabolic transformation of AZA1 using the same system, and therefore this compound is the known mussel metabolite AZA13 (Figure 1).

Metabolism of AZAs. The metabolism observed in this study was closely aligned with that which has been described previously in mussels.[10] In particular, the 22-Me group present in AZA1 and AZA2 was oxidized to form 22α-carboxyAZAs AZA17 and AZA18, which have previously been shown to undergo thermal decarboxylation to yield 22-demethylAZAs AZA3 and AZA6.[38, 50] It should be noted that although brief heating was used to induce decarboxylation in this and previous studies,[38] we also observed significant decarboxylation of AZA17 to give AZA3 when an MeCN extract from metabolism of AZA1 was stored for several weeks at ambient temperature (~20 °C). Clearly, this decarboxylation occurs spontaneously even at room temperature, although the rate is accelerated by increasing temperature. This probably accounts

for the presence of 22-demethylAZAs and their metabolites detected in the in vitro metabolism experiments with the HP-fractions, as well as in mussels naturally contaminated with AZAs.

Previous studies have not reported any intermediates between the 22-methylAZAs AZA1 and AZA2, and their 22α-carboxy derivatives AZA17 and AZA19. In this study, we observed major metabolites that LC–HRMS/MS unambiguously showed to be 22α-hydroxymethylAZAs AZA65 and AZA66, which have not previously been identified in contaminated shellfish or in *Azadinium* cultures. Given that AZA65 and AZA66 are intermediate in their oxidation states at their C-22-substituent between precursors AZA1 and AZA2 and metabolites AZA17 and AZA19, AZA65 and AZA66 are highly likely to be intermediates in the known metabolic conversion of AZA1 and AZA2 into AZA17 and AZA18, which is then followed by spontaneous decarboxylation to AZA3 and AZA6 (Figure 4). In this study, AZA3 was metabolized predominantly to its 23α-hydroxy derivative (AZA5), and the only other significant hydroxylation product was 3β-hydroxyAZA3 (AZA4), with traces of the 3β,23α-dihydroxyAZA3 (AZA13) being formed, and as with AZA1 and AZA2, 3β-hydoxylation appeared to be much slower than 23α-hydroxylation for AZA3.

The only carboxylic acid derivatives observed in this study were AZA17 and AZA18, produced by oxidative metabolism of AZA1 and AZA2, respectively. No carboxylic acid derivatives of AZA3 were detected which, together with observations for AZA1 and AZA2, indicates that the 22-Me group is strongly favored as the site for oxidative metabolism in the blue mussel HP-fraction. This is in accord with the metabolites that have so far been detected in naturally contaminated blue mussels. However, novel broad, early-eluting peaks of oxidized AZAs AZA(872), AZA(886), and AZA(858) were observed as metabolites of AZA1–3, respectively, which had the same accurate mass as expected for their respective carboxylic acid derivatives (Figures 2, S4 and S5). Analysis of the LC–HRMS/MS data for the three metabolites (Figures 5, 7, 8, and S6) showed that oxidation has occurred between C-16 and C-27, does not depend on the presence of a 22-Me group, does not appear to involve formation of a carboxylic

450 acid group, and results in the formation of a novel HRMS/MS product ion containing C-22–C-
451 40 and appended substituents. While the structure of this new group of metabolites is only
452 partially determined, their chromatographic and mass spectral characteristics suggest (as
453 discussed in more detail above for AZA(872)) the insertion of ketones or aldehydes, along with
454 possible opening of the E-ring that is normally closed by a hemiketal linkage at C-21 in
455 precursors AZA1–3. Full identification of these metabolites will require additional studies,
456 possibly including purification and structure elucidation by NMR spectroscopy. Their presence
457 also serves as a reminder that it is unsafe to assume that all AZAs will fragment in a similar
458 manner to the more familiar AZAs such as AZA1 and AZA2, and that it would be wise to include
459 a wider array of cleavages, such as cleavages I–K, in addition to cleavage G (Figure 3), when
460 searching MS/MS spectra for candidate AZA analogues and metabolites in natural samples.
461 Comparison with an extract from highly contaminated blue mussels from Bruckless,
462 Ireland, showed significant differences to the metabolite profiles found in our in vitro study
463 (Figures S10 and S15–S19). The main differences were that a much lower proportion of 3β-
464 hydroxylation and 22α-hydroxymethyl oxidation (to 22α-carboxy) were apparent in vitro, such
465 that a relatively low proportion of AZA7 and high proportion of AZA65 accumulated when
466 AZA1 was metabolized in vitro, compared to naturally contaminated mussels. Nevertheless,
467 AZA65–AZA68, and AZA(872) were identified by LC–HRMS/MS (method A) at low levels in
468 naturally contaminated blue mussels and in two mussel tissue reference materials based on their
469 retention times (Figures S10 and S15–S19) and HRMS/MS spectra. The presence of novel AZAs
470 AZA65–AZA68, and AZA(872) in CRM-FDMT1 was confirmed by comparison with the
471 metabolized samples (Figures S7 and S20–S24) using a second analytical method, LC–
472 HRMS/MS (method B), which included application of PRM and DDA methods to acquire
473 HRMS/MS spectra. The presence of AZA65–AZA68, AZA(872), and AZA(886) in tissue
474 reference materials (Figures S7, S10, and S15–S24) will facilitate the confirmation of these
475 metabolites in shellfish and algae by other researchers.

Previous work found that ELISA analysis of AZAs in shellfish, using an antibody that recognizes only the ring-F–I substructure, gave concentrations significantly higher than targeted LC–MS/MS methods, even when AZA1–10 were included in the LC–MS/MS method.[61] However, the broader array of AZA metabolites being revealed in mussels by modern untargeted LC–MS techniques, such as those identified here, and in other studies[10, 44, 57, 62] provide a plausible explanation for this difference. This is because all the metabolites identified to-date in shellfish contain the rings-F–I substructure that is recognized by the antibodies, but not all are detected with routine LC–MS/MS methods. Previous studies suggest that the in vitro toxicity of AZAs resides primarily in rings E–I,[10, 54] so it would be interesting to have toxicological data on some of the new metabolites such as AZA65–AZA68, AZA(872), AZA(886), and AZA(858) given that AZA65–AZA68, AZA(872), and AZA(886) were also detected in mussel samples.

In addition to providing valuable new information about the metabolism of AZAs, this study also showed that it is potentially possible to efficiently convert AZAs into blue mussel metabolites in vitro. Thus far, shellfish metabolites of AZAs, such as AZA3–10, have had to be laboriously isolated from contaminated shellfish.[52] AZA1 and AZA2 can be efficiently produced in algal culture,[41, 54] so if the in vitro metabolism procedure can be scaled up, then practical routes to the production of AZA metabolites will become available for production of standards. These would be invaluable for use in analytical method development and validation, toxicological studies, and other areas of research. This approach may also prove useful for providing metabolites of other classes of marine algal toxins.

ASSOCIATED CONTENT

Supporting Information

LC–HRMS/MS chromatograms (methods A–C) and HRMS/MS spectra (method A) of AZAs from standards, reference materials, stock solutions, and samples metabolised by the hepatopancreatic fraction, and a tabulation of observed product ions. This material is available free of charge via the Internet at http://...

AUTHOR INFORMATION

Corresponding Author

* Tel.: +47-911-79-138; e-mail: ingunn.samdal@vetinst.no

Funding

This work was carried out as part of the MARBioFEED project, supported under the First Call for Transnational Research Projects within the Marine Biotechnology ERA-NET; project no. 604814 ("Enhanced Biorefining Methods for the Production of Marine Biotoxins and Microalgae Fish Feed"), funded partly by the Norwegian Research Council.

Notes

The authors declare no competing financial interest.

ACKNOWLEDGEMENTS

The authors would like to Christiane K. Fæste (Norwegian Veterinary Institute, Ås, Norway), and Pearse McCarron (National Research Council, Halifax, Canada), for critical reviews of the manuscript, and Samantha L. Dudra (National Research Council, Halifax, Canada) for assistance with some of the shellfish tissue extractions.

ABBREVIATIONS

AZA, azaspiracid; HP, hepatopancreas; LC–HRMS, Liquid Chromatography–High Resolution Mass Spectrometry

REFERENCES

(1) McMahon, T.; Silke, J., Winter toxicity of unknown aetiology in mussels. *Harmful Algae News* **1996,** *14*, 2.

(2) Twiner, M. J.; Hess, P.; Doucette, G. J., Azaspiracids: toxicology, pharmacology, and risk assessment. In *Seafood and Freshwater Toxins. Phamacology, Physiology, and Detection*, 3rd ed.; Botana, L. M., Ed. CRC Press: Boca Raton, FL, 2014; pp 823–856.

(3) Satake, M.; Ofuji, K.; Naoki, H.; James, K. J.; Furey, A.; McMahon, T.; Silke, J.; Yasumoto, T., Azaspiracid, a new marine toxin having unique spiro ring assemblies, isolated from Irish mussels, *Mytilus edulis*. *J. Am. Chem. Soc.* **1998,** *120*, 9967–9968.

(4) FAO/IOC/WHO *Report of the joint FAO/IOC/WHO ad hoc expert consultation on biotoxins in bivalve molluscs*; Oslo, Norway, 26.-30. Sept. 2004, 2004; p 40. http://www.fao.org/3/au629e/au629e.pdf (accessed on 15.04.2021).

(5) Ofuji, K.; Satake, M.; McMahon, T.; Silke, J.; James, K. J.; Naoki, H.; Oshima, Y.; Yasumoto, T., Two analogs of azaspiracid isolated from mussels, *Mytilus edulis*, involved in human intoxication in Ireland. *Nat. Toxins* **1999,** *7*, 99–102.

(6) Nicolaou, K. C.; Koftis, T. V.; Vyskocil, S.; Petrovic, G.; Ling, T. T.; Yamada, Y. M. A.; Tang, W. J.; Frederick, M. O., Structural revision and total synthesis of azaspiracid-1, part 2: Definition of the ABCD domain and total synthesis. *Angew. Chem. Int. Ed.* **2004,** *43*, 4318–4324.

(7) Nicolaou, K. C.; Vyskocil, S.; Koftis, T. V.; Yamada, Y. M. A.; Ling, T. T.; Chen, D. Y. K.; Tang, W. J.; Petrovic, G.; Frederick, M. O.; Li, Y. W.; Satake, M., Structural revision and total synthesis of azaspiracid-1, part 1: Intelligence gathering and tentative proposal. *Angew. Chem. Int. Ed.* **2004,** *43*, 4312–4318.

(8) Kenton, N. T.; Adu-Ampratwum, D.; Okumu, A. A.; McCarron, P.; Kilcoyne, J.; Rise, F.; Wilkins, A. L.; Miles, C. O.; Forsyth, C. J., Stereochemical definition of the natural product (6*R*,10*R*,13*R*,14*R*,16*R*,17*R*,19*S*,20*S*,21*R*,24*S*,25*S*,28*S*,30*S*,32*R*,33*R*,34*R*,36*S*,37*S*,39*R*)-azaspiracid-3 via total synthesis and comparative analyses. *Angew. Chem. Int. Ed.* **2018,** *57*, 810–813.

(9) Kenton, N. T.; Adu-Ampratwum, D.; Okumu, A. A.; Zhang, Z.; Chen, Y.; Nguyen, S.; Xu, J.; Ding, Y.; McCarron, P.; Kilcoyne, J.; Rise, F.; Wilkins, A. L.; Miles, C. O.; Forsyth, C. J., Total synthesis of (6*R*,10*R*,13*R*,14*R*,16*R*,17*R*,19*S*,20*R*,21*R*,24*S*,25*S*,28*S*,30*S*,32*R*,33*R*,34*R*,36*S*,37*S*,39*R*)-azaspiracid-3 reveals non-identity with the natural product. *Angew. Chem. Int. Ed.* **2018,** *57*, 805–809.

(10) Kilcoyne, J.; McCarron, P.; Twiner, M. J.; Rise, F.; Hess, P.; Wilkins, A. L.; Miles, C. O., Identification of 21,22-dehydroazaspiracids in mussels (*Mytilus edulis*) and in vitro toxicity of azaspiracid-26. *J. Nat. Prod.* **2018,** *81*, 885–893.

(11) Krock, B.; Tillmann, U.; Tebben, J.; Trefault, N.; Gu, H., Two novel azaspiracids from *Azadinium poporum*, and a comprehensive compilation of azaspiracids produced by *Amphidomataceae*, (Dinophyceae). *Harmful Algae* **2019,** *82*, 1-8.

(12) Kilcoyne, J.; McCoy, A.; Burrell, S.; Krock, B.; Tillmann, U., Effects of temperature, growth media, and photoperiod on growth and toxin production of *Azadinium spinosum*. *Mar. Drugs* **2019,** *17*, 489.

(13) Krock, B.; Tillmann, U.; John, U.; Cembella, A. D., Characterization of azaspiracids in plankton size-fractions and isolation of an azaspiracid-producing dinoflagellate from the North Sea. *Harmful Algae* **2009,** *8*, 254–263.

(14) Tillmann, U.; Elbrachter, M.; Krock, B.; John, U.; Cembella, A. D., *Azadinium spinosum* gen. et sp. nov. (Dinophyceae) identified as a primary producer of azaspiracid toxins. *Eur. J. Phycol.* **2009,** *44*, 63–79.

(15) Krock, B.; Tillmann, U.; Voß, D.; Koch, B. P.; Salas, R.; Witt, M.; Potvin, É.; Jeong, H. J., New azaspiracids in *Amphidomataceae* (Dinophyceae). *Toxicon* **2012,** *60*, 830−839.
(16) Krock, B.; Tillmann, U.; Witt, M.; Gu, H., Azaspiracid variability of *Azadinium poporum* (Dinophyceae) from the China Sea. *Harmful Algae* **2014,** *36*, 22−28.
(17) Hess, P.; McCarron, P.; Krock, B.; Kilcoyne, J.; Miles, C. O., Azaspiracids: chemistry, biosynthesis, metabolism, and detection. In *Seafood and Freshwater Toxins. Phamacology, Physiology, and Detection*, 3rd ed.; Botana, L. M., Ed. CRC Press: Boca Raton, FL, 2014; pp 799−822.
(18) Aasen, J. A. B.; Torgersen, T.; Dahl, E.; Naustvoll, L. J.; Aune, T., Confirmation of azaspiracids in mussels in Norwegian coastal areas, and full profile at one location. In *Proceedings of 5th International Conference on Molluscan Shellfish Safety in 2004*, Henshilwood, K.; Deegan, B.; McMahon, T.; Cusack, C.; Keaveney, S.; Silke, J.; O' Cinneide, M.; Lyons, D.; Hess, P., Eds. Galway, Ireland, 2006; pp 162−169.
(19) James, K. J.; Furey, A.; Lehane, M.; Ramstad, H.; Aune, T.; Hovgaard, P.; Morris, S.; Higman, W.; Satake, M.; Yasumoto, T., First evidence of an extensive northern European distribution of azaspiracid poisoning (AZP) toxins in shellfish. *Toxicon* **2002,** *40*, 909−915.
(20) Magdalena, A. B.; Lehane, M.; Krys, S.; Fernandez, M. L.; Furey, A.; James, K. J., The first identification of azaspiracids in shellfish from France and Spain. *Toxicon* **2003,** *42*, 105−108.
(21) Furey, A.; Moroney, C.; Magdalena, A. B.; Saez, M. J. F.; Lehane, M.; James, K. J., Geographical, temporal, and species variation of the polyether toxins, azaspiracids, in shellfish. *Environ. Sci. Technol.* **2003,** *37*, 3078−3084.
(22) Amzil, Z.; Sibat, M.; Royer, F.; Savar, V., First report on azaspiracid and yessotoxin groups detection in French shellfish. *Toxicon* **2008,** *52*, 39−48.
(23) Torgersen, T.; Bremnes, N. B.; Rundberget, T.; Aune, T., Structural confirmation and occurrence of azaspiracids in Scandinavian brown crabs (*Cancer pagurus*). *Toxicon* **2008,** *51*, 93−101.
(24) Taleb, H.; Vale, P.; Amanhir, R.; Benhadouch, A.; Sagou, R.; Chafik, A., First detection of azaspiracids in mussels in north west Africa. *J. Shellfish Res.* **2006,** *25*, 1067−1070.
(25) Twiner, M. J.; Rehmann, N.; Hess, P.; Doucette, G. J., Azaspiracid shellfish poisoning: a review on the chemistry, ecology, and toxicology with an emphasis on human health impacts. *Mar. Drugs* **2008,** *6*, 39−72.
(26) Alvarez, G.; Uribe, E.; Avalos, P.; Marino, C.; Blanco, J., First identification of azaspiracid and spirolides in *Mesodesma donacium* and *Mulinia edulis* from northern Chile. *Toxicon* **2010,** *55*, 638−641.
(27) Lopez-Rivera, A.; O'Callaghan, K.; Moriarty, M.; O'Driscoll, D.; Hamilton, B.; Lehane, M.; James, K. J.; Furey, A., First evidence of azaspiracids (AZAs): a family of lipophilic polyether marine toxins in scallops (*Argopecten purpuratus*) and mussels (*Mytilus chilensis*) collected in two regions of Chile. *Toxicon* **2010,** *55*, 692−701.
(28) Liu, Y.; Yu, R. C.; Kong, F. Z.; Li, C.; Dai, L.; Chen, Z. F.; Geng, H. X.; Zhou, M. J., Contamination status of lipophilic marine toxins in shellfish samples from the Bohai Sea, China. *Environ. Pollut.* **2019,** *249*, 171−180.
(29) Kim, J.-H.; Tillmann, U.; Adams, N. G.; Krock, B.; Stutts, W. L.; Deeds, J. R.; Han, M.-S.; Trainer, V. L., Identification of *Azadinium* species and a new azaspiracid from *Azadinium poporum* in Puget Sound, Washington State, USA. *Harmful Algae* **2017,** *68*, 152−167.
(30) Ueoka, R.; Ito, A.; Izumikawa, M.; Maeda, S.; Takagi, M.; Shin-ya, K.; Yoshida, M.; van Soest, R.; Matsunaga, S., Isolation of azaspiracid-2 from a marine sponge *Echinoclathria* sp. as a potent cytotoxin. *Toxicon* **2009,** *53*, 680−684.
(31) Munday, R., Toxicology of seafood toxins: a critical review. In *Seafood and Freshwater Toxins. Phamacology, Physiology, and Detection*, 3rd ed.; Botana, L. M., Ed. CRC Press: Boca Raton, FL, 2014; pp 197−290.

(32) Ito, E.; Satake, M.; Ofuji, K.; Higashi, M.; Harigaya, K.; McMahon, T.; Yasumoto, T., Chronic effects in mice caused by oral administration of sublethal doses of azaspiracid, a new marine toxin isolated from mussels. *Toxicon* **2002,** *40*, 193–203.
(33) Ito, E.; Satake, M.; Ofuji, K.; Kurita, N.; McMahon, T.; James, K.; Yasumoto, T., Multiple organ damage caused by a new toxin azaspiracid, isolated from mussels produced in Ireland. *Toxicon* **2000,** *38*, 917–930.
(34) Ito, E.; Frederick, M. O.; Koftis, T. V.; Tang, W.; Petrovic, G.; Ling, T.; Nicolaou, K. C., Structure toxicity relationships of synthetic azaspiracid-1 and analogs in mice. *Harmful Algae* **2006,** *5*, 586–591.
(35) Colman, J. R.; Twiner, M. J.; Hess, P.; McMahon, T.; Satake, M.; Yasumoto, T.; Doucette, G. J.; Ramsdell, J. S., Teratogenic effects of azaspiracid-1 identified by microinjection of Japanese medaka (*Oryzias latipes*) embryos. *Toxicon* **2005,** *45*, 881–890.
(36) Alfonso, A.; Vieytes, M. R.; Ofuji, K.; Satake, M.; Nicolaou, K. C.; Frederick, M. O.; Botana, L. M., Azaspiracids modulate intracellular pH levels in human lymphocytes. *Biochem. Biophys. Res. Commun.* **2006,** *346*, 1091–1099.
(37) Twiner, M. J.; Doucette, G. J.; Rasky, A.; Huang, X.-P.; Roth, B. L.; Sanguinetti, M. C., Marine algal toxin azaspiracid is an open-state blocker of hERG potassium channels. *Chem. Res. Toxicol.* **2012,** *25*, 1975–1984.
(38) McCarron, P.; Kilcoyne, J.; Miles, C. O.; Hess, P., Formation of azaspiracids -3, -4, -6, and -9 via decarboxylation of carboxyazaspiracid metabolites from shellfish. *J. Agric. Food Chem.* **2009,** *57*, 160–169.
(39) Jauffrais, T.; Kilcoyne, J.; Herrenknecht, C.; Truquet, P.; Sechet, V.; Miles, C. O.; Hess, P., Dissolved azaspiracids are absorbed and metabolized by blue mussels (*Mytilus edulis*). *Toxicon* **2013,** *65*, 81–89.
(40) Salas, R.; Tillmann, U.; John, U.; Kilcoyne, J.; Burson, A.; Cantwell, C.; Hess, P.; Jauffrais, T.; Silke, J., The role of *Azadinium spinosum* (Dinophyceae) in the production of azaspiracid shellfish poisoning in mussels. *Harmful Algae* **2011,** *10*, 774–783.
(41) Jauffrais, T.; Herrenknecht, C.; Sechet, V.; Sibat, M.; Tillmann, U.; Krock, B.; Kilcoyne, J.; Miles, C. O.; McCarron, P.; Amzil, Z.; Hess, P., Quantitative analysis of azaspiracids in *Azadinium spinosum* cultures. *Anal. Bioanal. Chem.* **2012,** *403*, 833–846.
(42) O'Driscoll, D.; Skrabakova, Z.; O'Halloran, J.; van Pelt, F. N. A. M.; James, K. J., Mussels increase xenobiotic (azaspiracid) toxicity using a unique bioconversion mechanism. *Environ. Sci. Technol.* **2011,** *45*, 3102–3108.
(43) Ji, Y.; Qiu, J.; Xie, T.; McCarron, P.; Li, A., Accumulation and transformation of azaspiracids in scallops (*Chlamys farreri*) and mussels (*Mytilus galloprovincialis*) fed with *Azadinium poporum*, and response of antioxidant enzymes. *Toxicon* **2018,** *143*, 20–28.
(44) Mudge, E. M.; Miles, C. O.; Hardstaff, W. R.; McCarron, P., Fatty acid esters of azaspiracids identified in mussels (*Mytilus edulis*) using liquid chromatography–high resolution mass spectrometry. *Toxicon: X* **2020,** *8*, 100059–100059.
(45) Kittler, K.; Preiss-Weigert, A.; These, A., Identification strategy using combined mass spectrometric techniques for elucidation of phase I and phase II *in vitro* metabolites of lipophilic marine biotoxins. *Anal. Chem.* **2010,** *82*, 9329–9335.
(46) EC, Regulation (EC) No 853/2004 of the European Parliament and of the Council of 29 April 2004 laying down specific hygiene rules for on the hygiene of foodstuffs. *Off. J. Eur. Commun.* **2004,** *L139*, 99–100.
(47) EC, Commission regulation (EU) No 15/2011 of 10 January 2011 amending Regulation (EC) No 2074/2005 as regards recognised testing methods for detecting marine biotoxins in live bivalve molluscs. *Off. J. Eur. Commun.* **2011,** *L6*, 3–6.
(48) Codex Alimentarius Commission *Standard for Live and Raw Bivalve Molluscs - Codex Stan 292-2008*; Codex Alimentarius Commission: Rome, 2008; pp 1–9.
http://www.fao.org/fao-who-codexalimentarius/sh-

proxy/en/?lnk=1&url=https%253A%252F%252Fworkspace.fao.org%252Fsites%252Fcodex%252FStandards%252FCXS%2B292-2008%252FCXS_292e_2015.pdf (accessed on 15.04.2021).
(49) EFSA, Marine biotoxins in shellfish – azaspiracid group. Scientific opinion of the panel on contaminants in the food chain. *The EFSA Journal* **2008,** *723*, 1–52.
(50) Kilcoyne, J.; McCarron, P.; Hess, P.; Miles, C. O., Effects of heating on proportions of azaspiracids 1–10 in mussels (*Mytilus edulis*) and identification of carboxylated precursors for azaspiracids 5, 10, 13, and 15. *J. Agric. Food Chem.* **2015,** *63*, 10980–10987.
(51) Vale, P.; Bire, R.; Hess, P., Confirmation by LC-MS/MS of azaspiracids in shellfish from the Portuguese north-western coast. *Toxicon* **2008,** *51*, 1449–1456.
(52) Kilcoyne, J.; Keogh, A.; Clancy, G.; LeBlanc, P.; Burton, I.; Quilliam, M.; Hess, P.; Miles, C. O., Improved isolation procedure for azaspiracids from shellfish, structural elucidation of azaspiracid-6, and stability studies. *J. Agric. Food Chem.* **2012,** *60*, 2447–2455.
(53) Kilcoyne, J.; Twiner, M. J.; McCarron, P.; Crain, S.; Giddings, S. D.; Foley, B.; Rise, F.; Hess, P.; Wilkins, A. L.; Miles, C. O., Structure elucidation, relative LC–MS and *in vitro* toxicity of azaspiracids 7–10 isolated from mussels (*Mytilus edulis*). *J. Agric. Food Chem.* **2015,** *63*, 5083–5091.
(54) Kilcoyne, J.; Nulty, C.; Jauffrais, T.; McCarron, P.; Herve, F.; Foley, B.; Rise, F.; Crain, S.; Wilkins, A. L.; Twiner, M. J.; Hess, P.; Miles, C. O., Isolation, structure elucidation, relative LC–MS response, and *in vitro* toxicity of azaspiracids from the dinoflagellate *Azadinium spinosum*. *J. Nat. Prod.* **2014,** *77*, 2465–2474.
(55) McCarron, P.; Giddings, S. D.; Reeves, K. L.; Hess, P.; Quilliam, M. A., A mussel (*Mytilus edulis*) tissue certified reference material for the marine biotoxins azaspiracids. *Anal. Bioanal. Chem.* **2015,** *407*, 2985-2996.
(56) McCarron, P.; Wright, E.; Emteborg, H.; Quilliam, M. A., A mussel tissue certified reference material for multiple phycotoxins. Part 4: certification. *Anal. Bioanal. Chem.* **2017,** *409*, 95–106.
(57) Wright, E. J.; McCarron, P., A mussel tissue certified reference material for multiple phycotoxins. Part 5: profiling by liquid chromatography–high-resolution mass spectrometry. *Anal. Bioanal. Chem.* **2021,** *413*, 2055–2069.
(58) Bio-Rad *DC protein assay instruction manual. LIT448 Rev D*; 2000; p 19. https://www.bio-rad.com/webroot/web/pdf/lsr/literature/LIT448.pdf (accessed on 26.02.2021).
(59) Rehmann, N.; Hess, P.; Quilliam, M. A., Discovery of new analogs of the marine biotoxin azaspiracid in blue mussels (*Mytilus edulis*) by ultra-performance liquid chromatography/tandem mass spectrometry. *Rapid Commun. Mass Spectrom.* **2008,** *22*, 549–558.
(60) Brombacher, S.; Edmonds, S.; Volmer, D. A., Studies on azaspiracid biotoxins. II. Mass spectral behavior and structural elucidation of azaspiracid analogs. *Rapid Commun. Mass Spectrom.* **2002,** *16*, 2306–2316.
(61) Samdal, I. A.; Løvberg, K. E.; Kristoffersen, A. B.; Briggs, L. R.; Kilcoyne, J.; Forsyth, C. J.; Miles, C. O., A practical ELISA for azaspiracids in shellfish via development of a new plate-coating antigen. *J. Agric. Food Chem.* **2019,** *67*, 2369–2376.
(62) Miles, C. O.; Kilcoyne, J.; McCarron, P.; Giddings, S. D.; Waaler, T.; Rundberget, T.; Samdal, I. A.; Løvberg, K. E., Selective extraction and purification of azaspiracids from blue mussels (*Mytilus edulis*) using boric acid gel. *J. Agric. Food Chem.* **2018,** *66*, 2962–2969.

718 **Table 1.** Percentage of AZA analogues present in specimens of AZA1, AZA2, and AZA3
719 metabolized by the HP-fraction from blue mussel hepatopancreas[a]

Azaspiracid analogue	AZA1		AZA2		AZA3	
	30 min	20 h	30 min	20 h	30 min	20 h
AZA1	92.9–95.1	5.7–34.7	ND	ND	ND	ND
AZA2	ND	ND	92.5–95.9	42.0–49.3	ND	ND
AZA3	1.7–2.4	13.3–21.6	ND	ND	87.9–94.6	12.1–25.1
AZA4	ND	ND	ND	ND	0.4–0.5	2.5–2.9
AZA5	ND	0.2–0.9	ND	ND	5.0–11.5	70.8–83.3
AZA6	ND	ND	1.4–2.3	16.5–18.2	ND	ND
AZA7	0.1	0.3–0.5	ND	ND	ND	ND
AZA8	0.7–1.0	10.7–15.2	ND	ND	ND	ND
AZA10	ND	ND	ND	0.3–0.4	ND	ND
AZA11	ND	ND	0.3	0.3	ND	ND
AZA12	ND	ND	0.6–1.0	7.0–7.9	ND	ND
AZA13	ND	ND	ND	ND	ND	0.3–0.5
AZA17	1.6–2.6	17.4–29.3	ND	ND	ND	ND
AZA19	ND	ND	1.5–2.7	20.5–23.3	ND	ND
AZA65	0.6–0.8	10.8–14.1	ND	ND	ND	ND
AZA66	ND	ND	0.3–1.1	3.2–4.2	ND	ND
AZA67	ND	0.3–0.6	ND	ND	ND	ND
AZA68	ND	ND	0.1	0.6–0.8	ND	ND
AZA(872)	0.1–0.2	8.8–15.7	ND	ND	ND	ND
AZA(886)	ND	ND	ND	2.7–3.4	ND	ND
AZA(858)	ND	ND	ND	ND	ND	1.3–1.8

720 [a]Ranges for three replicates (except only two replicates for AZA2 at 20 h) at each time point.
721 Concentrations are estimated from the areas under peaks in full-scan extracted ion (±5 ppm)
722 LC–HRMS (method A) chromatograms, assuming identical response factors. ND, not detected.

723

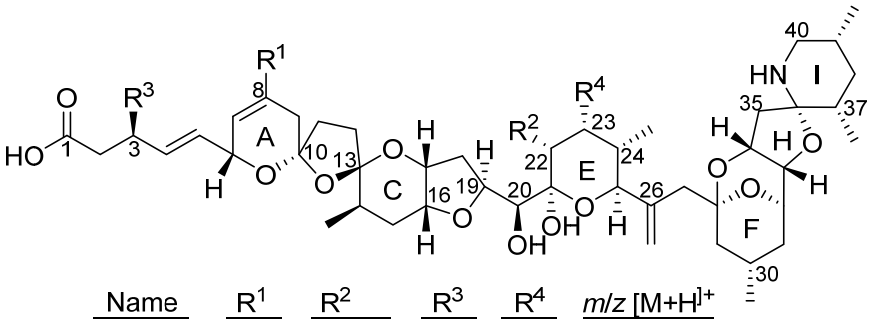

Name	R^1	R^2	R^3	R^4	*m/z* $[M+H]^+$
AZA1	H	CH_3	H	H	842.5049
AZA2	CH_3	CH_3	H	H	856.5206
AZA3	H	H	H	H	828.4893
AZA4	H	H	OH	H	844.4842
AZA5	H	H	H	OH	844.4842
AZA6	CH_3	H	H	H	842.5049
AZA7	H	CH_3	OH	H	858.4998
AZA8	H	CH_3	H	OH	858.4998
AZA9	CH_3	H	OH	H	858.4998
AZA10	CH_3	H	H	OH	858.4998
AZA11	CH_3	CH_3	OH	H	872.5155
AZA12	CH_3	CH_3	H	OH	872.5155
AZA13	H	H	OH	OH	860.4791
AZA14	H	CH_3	OH	OH	874.4947
AZA15	CH_3	H	OH	OH	874.4947
AZA16	CH_3	CH_3	OH	OH	888.5104
AZA17	H	CO_2H	H	H	872.4791
AZA19	CH_3	CO_2H	H	H	886.4947
AZA21	H	CO_2H	OH	H	888.4740
AZA23	CH_3	CO_2H	OH	H	902.4896
AZA65	H	CH_2OH	H	H	858.4998
AZA66	CH_3	CH_2OH	H	H	872.5155
AZA67	H	CH_2OH	H	OH	874.4947
AZA68	CH_3	CH_2OH	H	OH	888.5104
AZA(872)	H	?	H	?	872.4791
AZA(886)	CH_3	?	H	?	886.4947
AZA(858)	H	?	H	?	858.4634

Figure 1. Structures of AZAs mentioned in the text, with variable functionality at R^1–R^4 (C-1, C-8, C-22, and C-23). Note that all *m/z* values are exact masses, and that for AZA(872), AZA(886), and AZA(858), the structures in the ring-E region are undetermined.

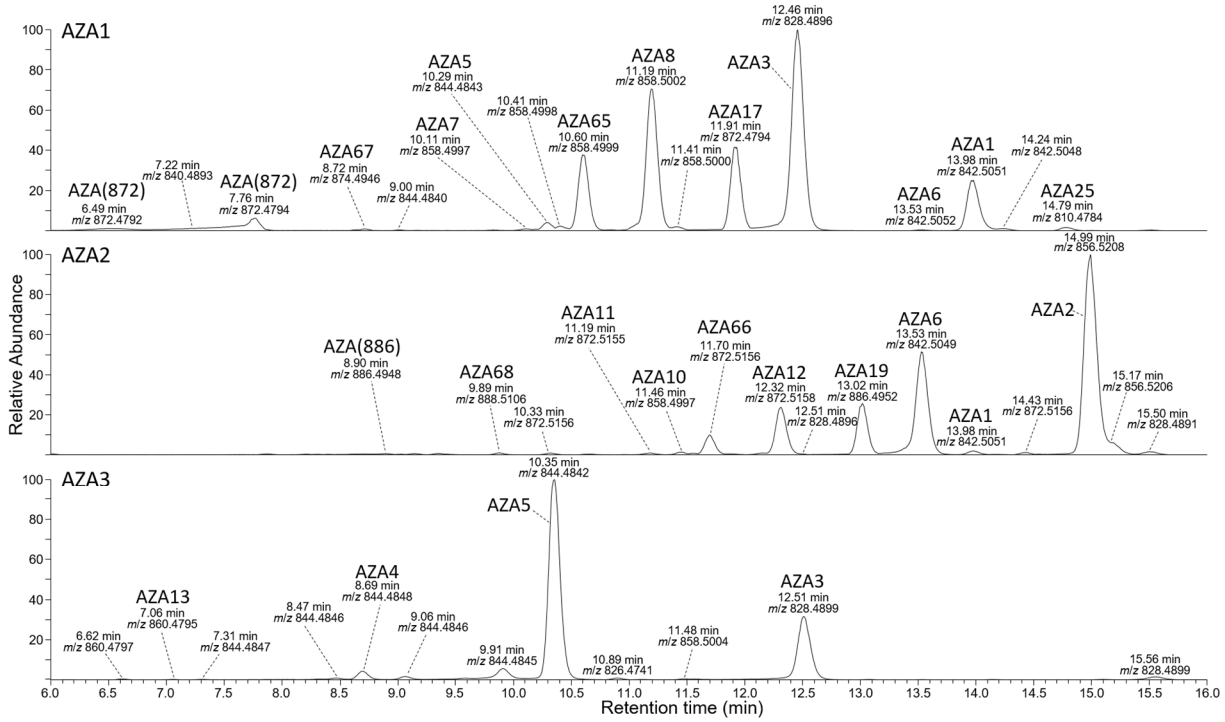

Figure 2. LC–HRMS (method A) base peak chromatograms (*m*/*z* 790–920) of extracts from metabolism (20 h) by the HP fraction of: top, AZA1; middle, AZA2 and; bottom, AZA3. Peaks are labeled with compound names (Figure 1), the retention time (min) and accurate mass (*m*/*z*). AZA(858) elutes at 2.7–4.9 min (main peak at 3.32 min, see Figure S4) and is not visible on the above AZA3-metabolism chromatogram.

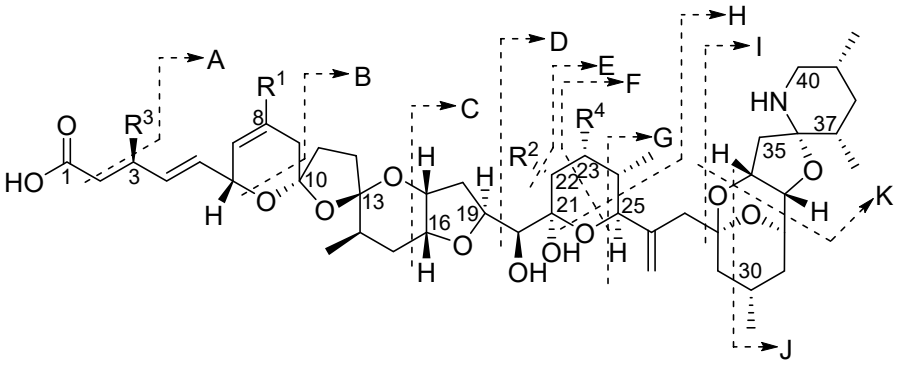

735

736 **Figure 3.** MS/MS fragmentations of AZAs observed during LC–HRMS/MS analyses (see
737 Figures 5–8 and Table S1). Note that fragmentations included losses of up to four water
738 molecules, and pathway A was only observed when R^3 = OH, fragmentation pathway E was
739 observed only with R^2 = CO_2H or CH_2OH, and fragmentation pathways F and H were only
740 observed when R^4 = OH.

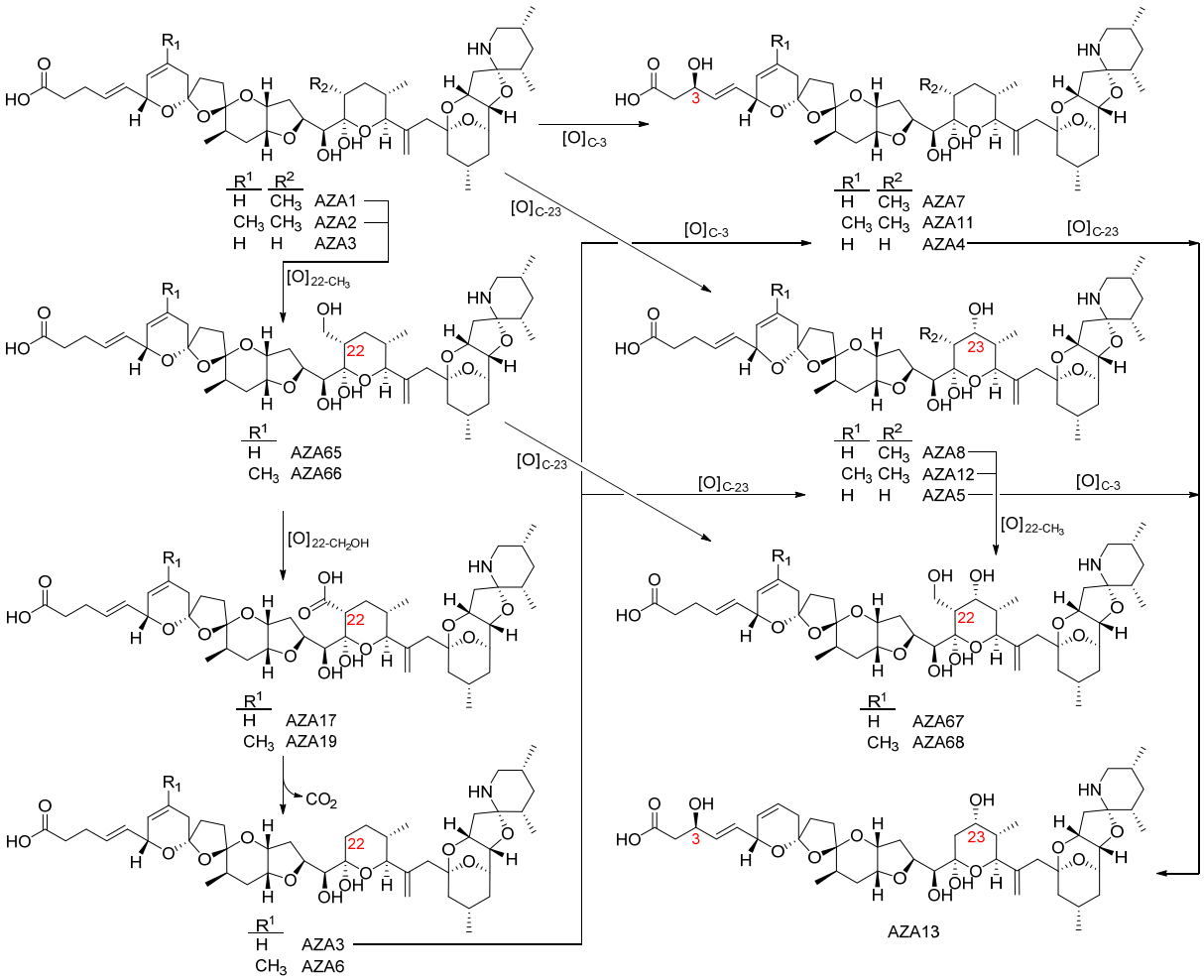

741

742 **Figure 4.** Proposed AZA interconversions observed for AZA1–3 in the HP-fraction isolated
743 from blue mussels (*M. edulis*). Note that AZA3 does not contain a 22-methyl group and so,
744 unlike AZA1 and AZA2, cannot undergo oxidative transformations at this position (reactions
745 shown in the left-hand column).

746

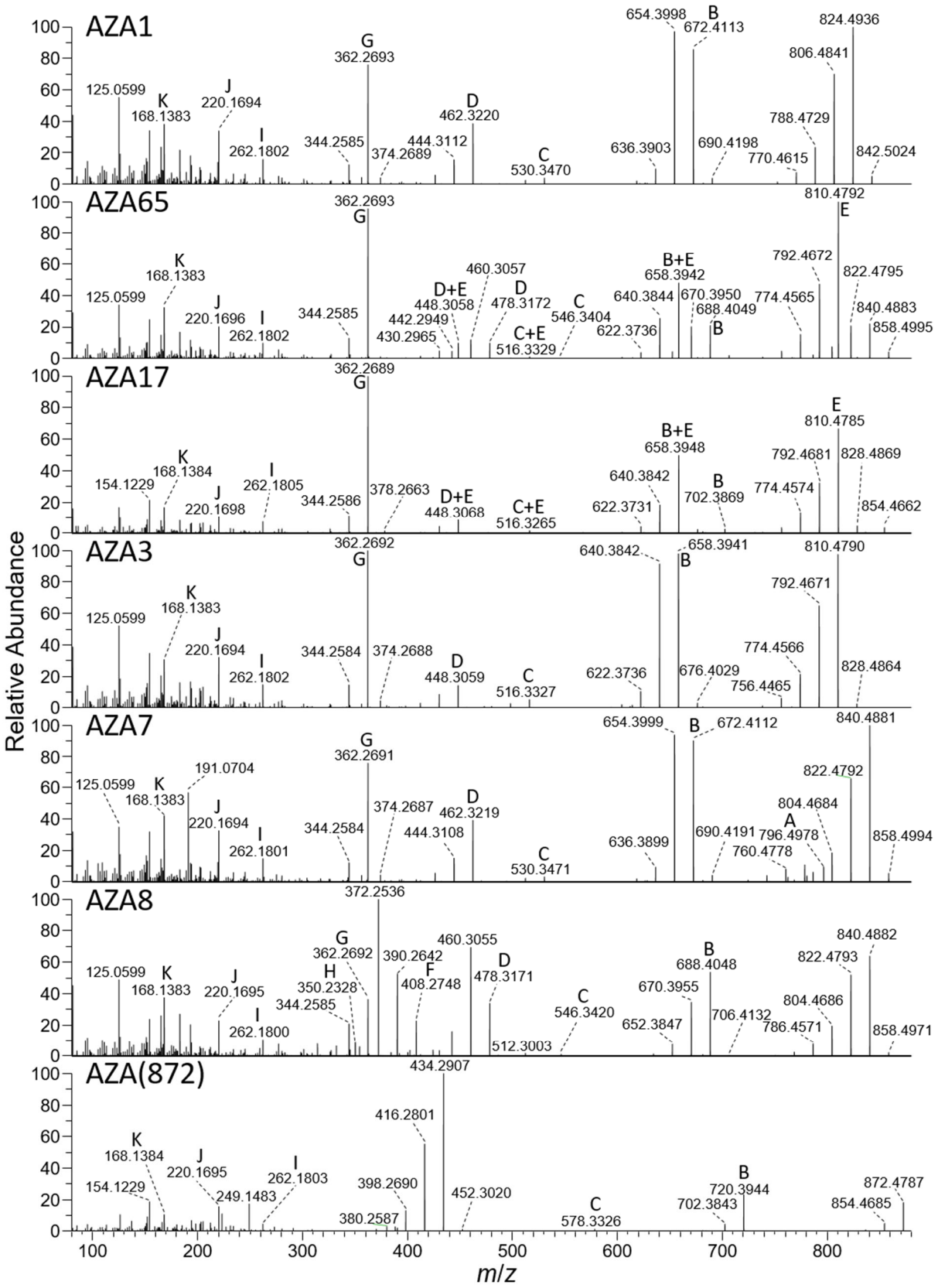

747

748 **Figure 5.** LC–HRMS/MS (method A) spectra of major components obtained during analysis of
749 an extract of AZA1 after incubation for 20 h with blue mussel the HP-fraction (Figures 2 and
750 4). Structures of the analytes are shown in Figure 1, and fragmentation pathways are shown in
751 Figure 3.

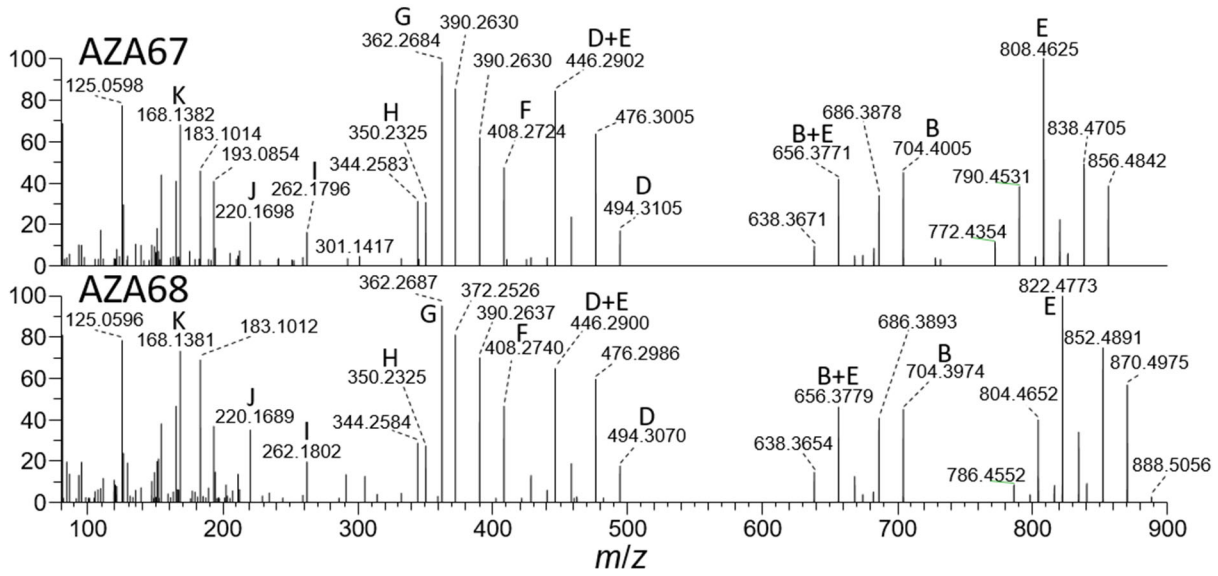

Figure 6. LC–HRMS/MS (method A) spectra of the identified minor components 22-hydroxymethyl-23-hydroxyAZA1 (AZA67) and 22-hydroxymethyl-23-hydroxyAZA2 (AZA68) obtained during analysis of an extract of AZA1 and AZA2 after incubation for 20 h with blue mussel the HP-fraction (Figures 2 and 4). Structures of the analytes are shown in Figure 1, and fragmentation pathways are shown in Figure 3.

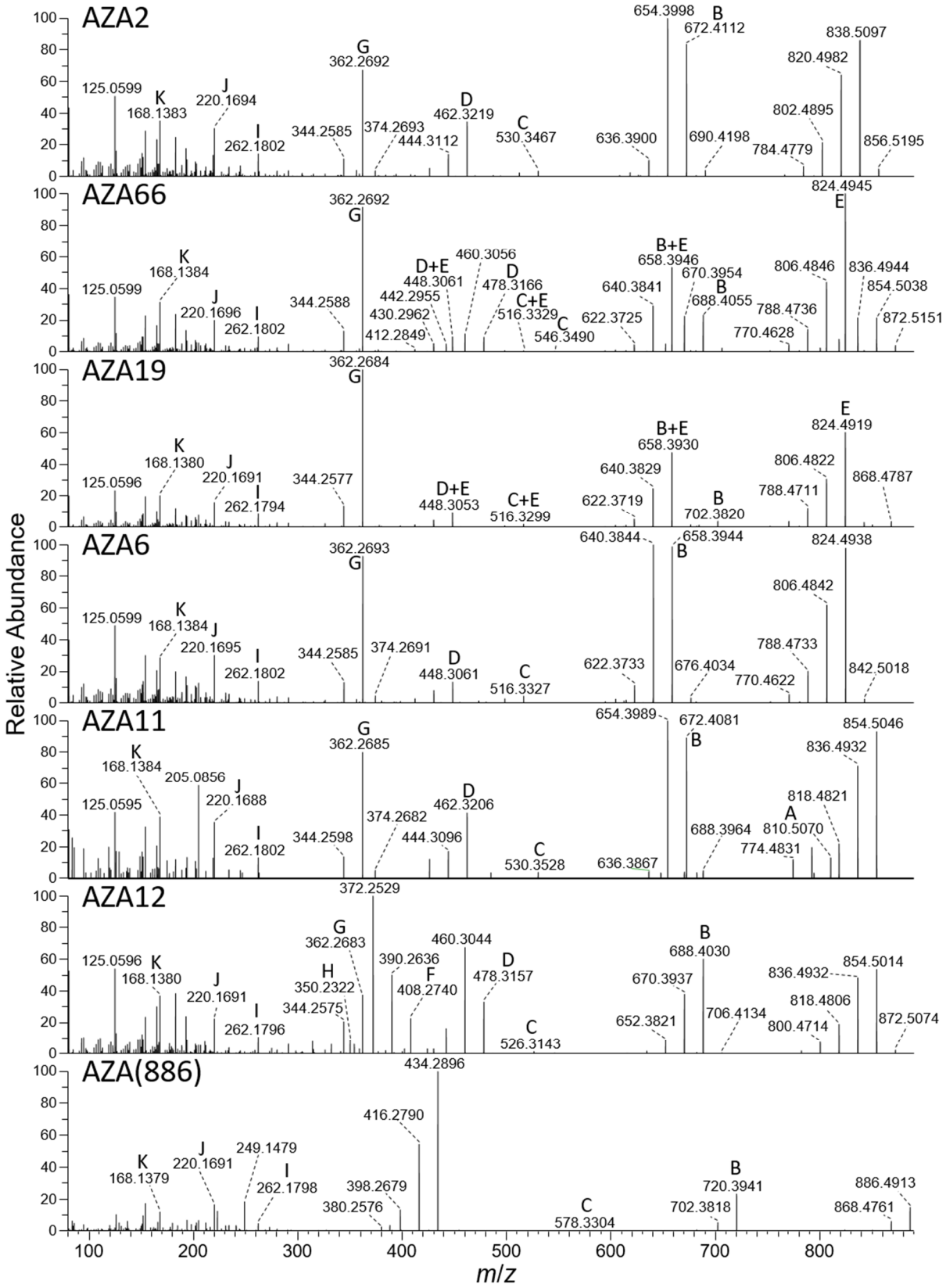

Figure 7. LC–HRMS/MS (method A) spectra of major components obtained during analysis of an extract of AZA2 after incubation for 20 h with blue mussel the HP-fraction (Figures 2 and 4). Structures of the analytes are shown in Figure 1, and fragmentation pathways are shown in Figure 3.

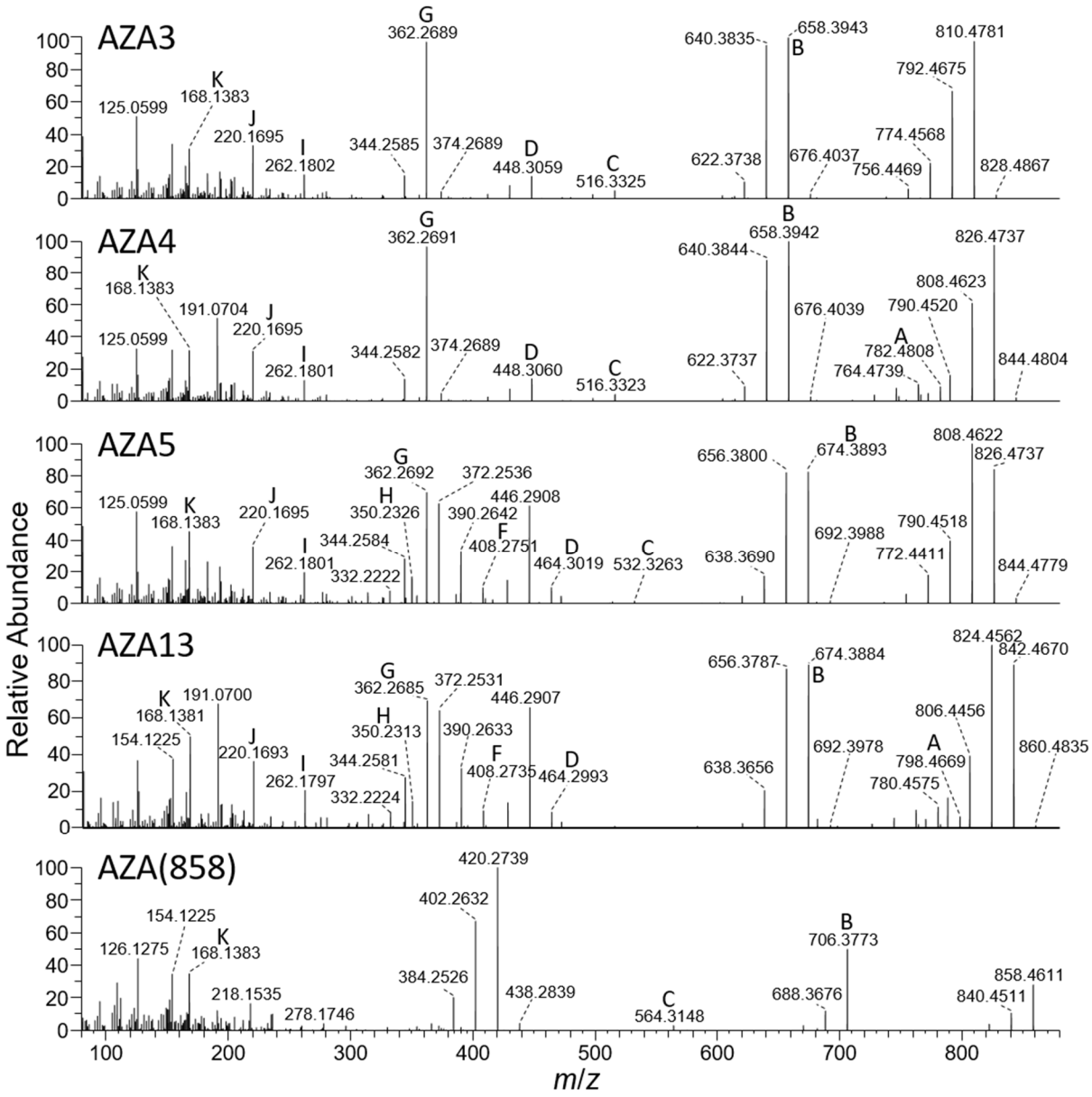

763

764 **Figure 8.** LC–HRMS/MS (method A) spectra of major components obtained during analysis of
765 an extract of AZA3 after incubation for 20 h with blue mussel the HP-fraction (Figures 2 and
766 4). Structures of the analytes are shown in Figure 1, and fragmentation pathways are shown in
767 Figure 3.
768

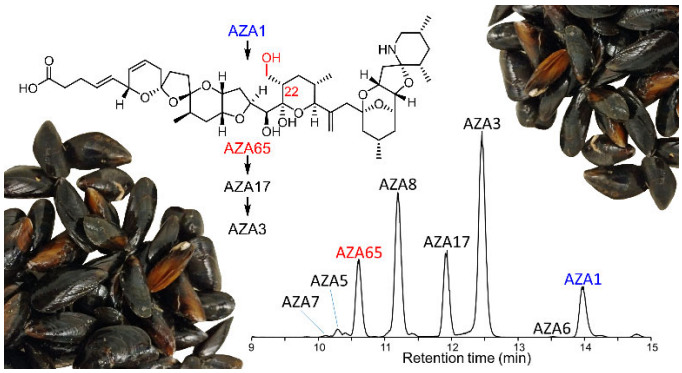

Table of Contents Graphic